A parametric study of cylindrical pedicle screw design implications on the pullout performance using an experimentally validated finite element model

Panagiotis E. Chatzistergos [(1)], Evangelos A. Magnissalis [(2)] and
Stavros K. Kourkoulis [(1), (*)]

(1) Unit of Biomechanics, Department of Mechanics, School of Applied Mathematical and Physical Sciences, National Technical University of Athens, Zografou Campus, Theocaris building, 157-73 Attiki, Greece

(2) Laboratory for the Research of the Musculoskeletal System (LRMS), University of Athens, KAT Hospital, Kifissia, Athens, Greece

(*) Corresponding author, tel.: + 30 210 7721263, fax: + 30 210 7721301,
e-mail: stakkour@central.ntua.gr

Abstract:

The present study aims to the design of a finite-element model simulating accurately the pullout behaviour of cylindrical pedicle screws and predicting their pullout force. Three commercial pedicle screws, subjected to pure pullout from synthetic bone, were studied experimentally. The results were used for the design, calibration and validation of a finite-element model. Special attention was paid to the accurate simulation of the failure inside the host material. For this purpose a bilinear cohesive zone material model was adopted to control mode-II debonding of neighbouring elements in the vicinity of the screw and simulate this way the failure in shear of the hosting material. Comparison between experimental and numerical results proved that the implementation of this method can significantly enhance the accuracy of the numerical simulation of a screw's mechanical behaviour under pure pullout loads. The numerical model was used for the parametric study of various factors affecting the pullout performance of a cylindrical pedicle screw. It was concluded that the major parameters influencing the pullout force is the outer radius and purchase length of the screw. Significantly weaker was the dependence of the screw's pullout force on its thread inclination, depth and pitch.

Keywords

Pedicle screws, Pullout force, Bilinear cohesive zone material model

Acknowledgements

This research project is co-financed by E.U.-European Social Fund (75%) and the Greek Ministry of Development-GSRT (25%).

1. Introduction

Spinal fixation with pedicle screws is one of the most commonly used methods of instrumentation in the thoracolumbar spine. Its greatest advantage is the achievement of immediate rigid fixation with a minimum number of fused segments. Despite this advantage and the technological advances of the last decades, implant failures of pedicle screw fixation still occur. The most common problems are screw bending, breakage and loosening [1-3]. Infection is also another implant-related complication.

From a purely engineering point of view, the above mentioned failures and complications could be confronted by optimizing the design of the pedicle screws in order to achieve higher stability and mechanical strength reducing at the same time the implant-bone interface area.

The strength of the fixation of a metallic medical bone screw can be quantified by measuring its pullout force. Even though pure pullout is a rather simple load case, unlikely to be applied in vivo [4], it helps enlightening some controversial points concerning the mechanical behaviour of the metallic screw - bone tissue system. The main factors affecting the pullout force of a bone screw are its design, the material properties of the bone and the insertion technique followed by the surgeon [5].

Especially for the screw design and its influence on the pullout force many experimental [6-18] and numerical [19-24] studies have been carried out. Additionally some researchers have attempted to quantify the factors that influence the pullout force of a bone screw using equations developed for “machine” screws (i.e. screws for traditional mechanical engineering use)[7,8]. However the pullout phenomenon has been proven more complex than it was initially anticipated and even today there is no accurate and reliable way to predict the pullout force of a bone screw [5].

Without any doubt, the best approach for a rigorous study of the influence of the screw's design on its pullout force is the combination of experimental investigation and numerical simulation of the pullout phenomenon using the Finite Element (FE) method.

In this context and for the purposes of the present study, the mechanical behaviour of two commercial cylindrical pedicle screws was investigated experimentally under pure pullout loads according to the respective standard (ASTM-F543-02). The experiments were performed using synthetic bone which simulated osteoporotic cancelous bone. The results of this experimental study were used for the design, calibration and validation of a reliable FE model which simulates the complex pullout failure mode and can accurately predict the pullout force of a pedicle screw. This FE model was employed for a thorough and detailed parametric study of the influence of the screw's design on its pullout force. The parameters studied were the outer radius, inclination, pitch and depth of the thread, as well as the screw purchase length. Another parameter that can influence a screw's pullout force is the conical angle of its core [22,23]. This parameter was not included to the present study which is focused on cylindrical screws.

2. Materials and methods

2.1. Experimental study

Three typical commercial pedicle screws were studied experimentally with respect to their pullout forces: The CDH 7.5, CDH 6.5 (Medtronic Sofamor Danek, Memphis, TN) and TL-Java5 (Zimmer Spine,Bordeaux,France). The basic quantities describing the geometry of the threads of these pedicle screws (Fig.1) are the outer radius (OR), the core radius (CR), the pitch (P), the thickness of the thread tip (e) and the inclination of the thread (a_1, a_2). It is seen in Table 1 that the two CDH screws differ only concerning OR and CR while all other parameters are identical, including the thread depth (D=OR-CR) while the TL-Java5 has a completely different thread design.

For the measurement of their pullout force, according to the ASTM-F543 standard, the pedicle screws were inserted into a Solid Rigid Polyurethane Foam (SRPF) block (10 pfc, Sawbones Worldwide, Pacific Research Laboratories Inc) fixed on the load cell (MTS 662.20D-04 Axial/Torsional Load Transducer) (Fig.2). The head of the screw was mounted on the loading frame (MTS MiniBionix 858, MTS Systems Corp., Eden Prairie, MN) and displacement was imposed in the pullout direction at a constant rate 0.01 mm/sec. The respective force was measured with a sampling rate of 10Hz.

The density of the SRPF used is 0.16g/cm^3, similar to osteoporotic cancelous bone [9,18]. Its mechanical properties are shown in Table 2. The main advantage of rigid polyurethane foam is the uniformity and consistency of its material properties which according to the ASTM F-1839: "makes it an ideal material for comparative testing of bone screws and other medical devises and instruments".

For the insertion of the screws into the SRPF blocks, guiding holes were drilled using a drill press. The radii of the guiding holes were about 60% of the respective core radius of the screw and their depth was 35mm. Before the screw insertion the cylindrical guiding holes were tapped manually in a manner consistent with surgical practice [26] using taps provided by the manufacturer. Finally the screws were inserted 25mm deep into the threaded holes. The guiding holes were drilled 10mm deeper than the desired screw insertion depth in order to ensure that the tip of the screw is not pressed against the bottom of the guiding hole, avoiding generation of undesired pretension into the SRPF.

The total number of threads inserted into the SRPF (N) was equal to 7 for the CDH screws and 11 for the TL-Java5 , which multiplied with the pitch of each screw (Table 1) yields the length of the threaded part of the screw inserted into the SRPF block equal to 18.9 mm and 19.25mm respectively. This length is referred as the purchase length of the screw (L).

2.2. FE model – Design, calibration, validation

The pullout phenomenon was simulated with a 2D axisymmetrical FE model (Fig.3), designed using the ANSYS11.0 software (ANSYS Inc., Canonsburg, PA, USA). The head and the tip of the screw were not included in the analysis. The FE model of the screw was placed into a threaded hole inside the respective model of the SRPF block (Fig.3). The hole was designed to have identical size and shape with the screw itself, simulating thus the insertion of the screw into a previously tapped threaded hole.

The model of the SRPF was meshed using 2D, 4-node FEs (Plane182). A rectangular area which surrounds the screw and includes the areas where high stresses are expected to be developed was meshed with a fine and uniform mesh. The remaining part of the SRPF model was meshed with a coarser non-uniform mesh. Several preliminary computational tests were performed, in order to define the optimum element size in the area surrounding the screw. Finally the value adopted was the one that ensured the mesh independency of the results with the minimum number of used elements. The total number of 2D plane elements was about 3000. The constitutive law of the SRPF was simulated by a linear elastic – perfectly plastic model based on data provided by the manufacturer (Table 2).

For the description of the failure inside the hosting material, the elements which lay in the vicinity of the screw were connected to each other using bonded contact elements (Conta171, Targe169). The mechanical behaviour of these bonded contact pairs was controlled by a bilinear cohesive zone material model [27] (Fig.4). According to this model, the tangential stress on the interface between a contact pair rises linearly (portion OA in Fig.4) until it reaches a critical value (τ_{max}), considered here equal to the shear yield stress of the SRPF (Table 2). From this point on increasing the relative sliding between the elements of the contact pair, results to a linear, non-reversible decrease of the tangential stress (branch AC in Fig.4). In this branch of the model unloading-reloading loops are realized along the OB line (Fig.4) indicating downgrading of the mechanical properties, i.e. appearance of internal damage. Finally, in case the relative sliding exceeds its critical value (u^c), complete debonding of the contact pair takes place and its behaviour is that of simple contact with friction [28].

In this way a series of parallel straight lines were formed along which relative sliding between neighbouring plain elements could occur (Fig.5), simulating this way the hosting material failure in shear. In three dimensions these straight lines correspond to cylindrical surfaces where one volume of SRPF can slide over another volume of SRPF, as it was observed experimentally.

The boundary conditions imposed on the surfaces between the screw and the SRPF were those of simple contact with friction and the value of the friction coefficient was set according to the literature [19,20] equal to 0.2.

The FE model of the SRPF block was constrained with a manner consistent to the experimental procedure previously described and a 3mm displacement was imposed to the screw; the value of the displacement chosen to be high enough to ensure that the SRPF will fail.

The imposition of the axisymmetrical conditions introduced to the analysis a new geometrical parameter: the distance ($x: 0<x<P$) between the first thread of the screw and the free surface of the SRPF block (Fig.3). The ratio x/P, where P is the screw pitch, was used for the calibration of the model. After a number of preliminary simulations, for the CDH7.5 screw, the value of x/P that minimizes the difference between the experimentally measured and numerically estimated pullout force was calculated. Finally the accuracy of the FE model was validated using the experimental results for the CDH6.5, TL-Java5 screws. The simulation was performed using the same value of the ratio x/P as previously.

2.3. Numerical study - Parametric scenarios

The parameters of the screw design considered in the present study were the outer radius (OR), the inclination, the depth (D) and the pitch (P) of the threads as well as their total number (N) and finally the purchase length (L) of the screw. The inclination of the thread is defined by two angles: a_1 and a_2 (Fig.1). For the load case of pure pullout only the inclination of the side of the thread that faces the pullout direction is able to influence the pullout force of the screw. For this reason only the influence of the angle a_1 was investigated here.

Each feature was isolated and its influence on the pullout force was evaluated separately. However the pitch, the total number of threads and the purchase length were studied in a combined manner, since they are interrelated. Indeed the purchase length is the product of pitch and total number of threads. Therefore, for the parametric study of the pitch the purchase length was kept constant, while for the investigation of the total number of threads the pitch was the parameter whose value was kept constant.

The results of these two parametric studies were finally used in an attempt to algebraically describe the relation between purchase length and pullout force.

The geometry of the CDH7.5 screw was used as the reference geometry. In every case (unless otherwise stated) when the influence of a single design parameter was investigated the values of the remaining ones were kept constant, equal to those of the CDH7.5 screw (Table 1). The combinations of the parameters studied (75 in total) as well as the calculated pullout force for each case studied are recapitulated in Table 3.

3. Results

3.1. Experimental study

The experimentally measured pullout forces for the CDH7.5, CDH6.5 and TL-Java5 screws were 438±2N, 382±3N and 315±4N respectively, while typical load vs. displacement curves are shown in Fig.6.

3.2. FE model – Design, calibration, validation

The results of the calibration procedure indicated that the pullout force increases linearly with increasing distance (x).The value of (x) that minimizes the difference between experimental and numerical pullout force for the CDH7.5 screw was calculated to be equal to 0.61P.

Using the same value for the parameter (x) the numerically estimated pullout forces for the CDH6.5 and TL-Java5 screws were 382.5 and 311.9N respectively resulting in a difference between experimental and numerical pullout force about 0.1%. In addition it is emphasized that the numerical model simulated in a very satisfactory manner the overall mechanical behaviour of the SRPF - screw system, as it is clearly concluded by comparing the experimental force - displacement curves with those obtained numerically (Fig.6).

Based on the above, one can safely conclude that the FE model, developed for the purposes of the present study, can estimate with satisfactory accuracy the pullout force of cylindrical screws inserted into SRPF blocks through previously tapped holes.

3.3. Numerical study – Parametric scenarios

3.3.1. General considerations on FE model

Prior to the study of individual parametric influences, the FE model was exploited to reveal stress distributions inside the SRPF bulk, able to highlight the SRPF – screw interface potential and performance. Indeed, it was shown that as the screw is pulled out of the SRPF block and the measured force rises (Fig.7A), strong stress concentrations appear near the edges of the threads (Fig.7B). The strongest concentration appears in the vicinity of the edge of the deepest thread, namely the one most distant from the free surface of the SRPF block. In other words it is indicated that the material in this region is the first to be challenged and consequently fail. The stress concentration is intensified until the force reaches its maximum value. At this point the tangential stress at one contact pair, of a previously defined line of possible relative sliding, reaches its critical value and debonding of neighbouring elements begins (Fig.7C). The areas where debonding takes place can be identified by the stress relief that follows it. In Fig.7D the stress relief due to debonding can be clearly seen around the edges of the three deepest threads.

The above mentioned remarks indicate that most of the pullout load is carried by the deepest threads (Fig.8). It is also indicated that the failure of the SRPF is initiated near the edge of the deepest thread of the SRPF and then propagates on a cylindrical surface towards the free boundary. This rationale of the failure seems to be a very good approximation of the respective one observed experimentally. Indeed, as it is seen in Fig.9, the failure of the SRPF occurs on an almost cylindrical surface which connects the edges of the threaded hole inside the SRPF. The material between the surface of failure and the surface of the screw was extracted from the block together with the screw.

Based on the above considerations regarding the natural history of SRPF – screw interfacial failure mode, individual parametric influences were demonstrated as follows (analytically exhibited in Table 3).

3.3.2 Influence of outer radius

The pullout force (F) clearly increases with the screw OR, following a strongly linear pattern:

$$F = 113.3 \cdot OR + 14.86, (R^2 = 1.00)$$

Increasing OR from 2.75 to 3.75 mm results to an increase of the pullout force from 280 to 375 N.

3.3.3 Influence of angle a_1

The pullout force depends weakly on angle a_1 following a strongly linear pattern:

$$F = 0.36 \cdot OR + 437.00, (R^2 = 1.00)$$

An increase of the a_1 angle of the thread from -5º to 25º resulted in an increase of the pullout force from 435N to 446N.

When nodal forces parallel to the pullout direction are calculated at failure initiation for the deepest SRPF thread, an influence by angle a_1 is also observed as follows: For sharp threads (a_1 = -5ºand 5 º) the pullout load peaks at the tip of the thread and clearly decreases towards the core; while for less sharp threads (a_1=25º) a similar but more moderate trend is followed (Fig.10).

3.3.4 Influence of thread depth

The pullout force, for sharp threads (a_1 = -5º and 5 º), clearly increases with thread depth from 0.5 to 0.75 mm, but remains relatively constant for higher values (Fig.11). However, the pullout force for less sharp thread (a_1=25°) demonstrates an almost linear increase throughout the thread depth range.

3.3.5 Influence of pitch, number of threads and purchase length

The pullout force, for constant purchase length, is insensitive (to within 3%) to changes of the pitch value, regardless of angle a_1, provided that the thread is relatively deep (D ≥ 0.75mm) (Figs.12A,B). However, for relatively shallow threads (D= 0.5mm), the pullout force is clearly decreasing with increasing pitch values beyond 1.89 mm and 2.70 mm for sharp (a_1=5°, Fig.12A) and less sharp threads (a_1=25°, Fig.12B), respectively.

The pullout force, for varying purchase lengths, is clearly increasing with the number of threads. Furthermore, this trend is accentuated with increasing pitch values (Fig.13). The equations which describe the linear correlation between the number of threads and the pullout force (F,unit:Newton) for different values of the thread pitch (N) are of the following form:

$$F = A_{(P)} \cdot N + B_{(P)} \qquad [1]$$

where $A_{(P)}$,$B_{(P)}$ are constants depending on the pitch (unit:mm).

From the results it was concluded that both constants are linearly depended on the value of the pitch:

$$A_{(P)} = 25.10 \cdot P - 2.69, (R^2 = 1.00) \qquad [2]$$

$$B_{(P)} = -10.48 \cdot P + 13.53, (R^2 = 0.97) \qquad [3]$$

By substituting equations [2],[3] and L=N·P into equation [1] the following equations are obtained:

$$F_{(L,P)} = \left(\frac{25.1 \cdot P - 2.7}{P} \right) \cdot L - 10.5 \cdot P + 13.5 \qquad [4]$$

$$F_{(L,N)} = \left(\frac{25.1 \cdot N - 10.5}{N} \right) \cdot L - 2.7 \cdot N + 13.5 \qquad [5]$$

where L is the screw's purcase length.

From these two equations it can be concluded that for constant pitch or number of threads the pullout force increases linearly with the purchace length.

4. Discussion and conclusions

Pedicle screws are sophisticated parts of structures exhibiting complex mechanical behaviour. The safest way to address this complexity is through the well known scheme of analysis and synthesis. In order to optimize the mechanical behaviour of pedicle screws one has to analyze it first, identify its different aspects, study each of these aspects separately and in the end synthesize the general solution from the partial ones. In this context, it can be noted that pedicle screws have a dual purely mechanical role:

a) to provide stability to the spinal fusion system by rigidly gripping itself into the vertebra and

b) to carry high loads vertical to its axis.

The present study is focused on the investigation of some factors affecting the strength of the pedicle screw fixation into the vertebra. The screws were studied under pure pullout loads. This load case was chosen because it helps to separate the strength of the screw's gripping from its mechanical behaviour under loads vertical to its axis.

The simplest solution to the problem of predicting the pullout force of a bone screw has been proposed by Lyon et al. [6] who in 1941 suggested that the pullout force is directly proportional to the volume of bone engaged by the screw's threads. Even though their strong correlation has been observed by numerous researchers [7,10-13], the direct proportionality has been proven to be an invalid hypothesis [14].
A more sophisticated approach has been proposed by Chapman et al. [7] and Asnis et al. [8] who used the formula provided by ASTM for the prediction of the "load to break threaded portion of screws and bolts"[29]. According to this formula the pullout force is proportional to the shear strength of the material into which the screw is inserted, it is proportional to the screw's outer radius and depth and inversely proportional to the screw's pitch. The shape of the threads is considered to have no influence on the pullout force. This formula has also been proven unable to entirely define the correlation between a screw's design and its pullout force [5]. It was also proven here that the pullout force is not proportional to the depth neither inverse proportional to the pitch of the screw.

In this context, the purpose of the present study was the development of a numerical instrument that will assist detailed parametric investigations of the influence of a pedicle screw's design on its holding power. During the first step of the present analysis, the mechanical behaviour of three typical commercial pedicle screws was studied experimentally according to the ASTM-F543. The results were used for the design of a FE model simulating accurately enough the mechanical behaviour of a cylindrical bone screw pulled out from a block of SRPF.

From the experiments, it became obvious that shearing is indeed the dominant failure mode inside the SRPF but it is not the only one. The material between the threads of the screw is compressed in a manner strongly depending on the shape and inclination of the threads. At the same time the material surrounding the tips of the threads is stretched. The stress field inside the SRPF is additionally influenced by the boundary conditions between the screw and the SRPF. These two materials are in simple contact with friction. Friction generates additional shear stresses along the sides of the threads while a possible relative sliding between screw and SRPF could also alter significantly the stress field inside the SRPF.

It is interesting to emphasize at this point that the number of numerical studies dealing with the investigation of the mechanical behaviour of a bone screw under pure pull-out loads is rather small [19-24] compared to the respective number of experimental studies. From these studies the only cases where a FE model was used for the prediction of the pullout force of different bone screws were those by Zhang et. al. [19,20]. The FE model developed by them simulated the behaviour of a pedicle screw pulled out from a rectangular volume of bone. For the design of this model two symmetry planes were considered by the authors, the bone was simulated as a linear elastic perfectly plastic material and the boundary conditions imposed on the interface between bone and screw were those of simple contact with friction. Finally the FE model was used for the parametric investigation of the influence of the purchase length, the pitch, the outer and core radius of the screw on its pullout force.

Since the pullout force corresponds to the instant at which failure of the SRPF occurs, the main consideration of the authors of the present study (during the design of the FE model of the screw - SRPF system), was to simulate as accurately as possible the failure of the SRPF. For this reason the SRPF was modelled as an isotropic, linearly elastic - perfectly plastic material and a surface-to-surface contact analysis was employed to simulate the boundary conditions between the screw and the SRPF. The originality of the present numerical analysis is the adoption of a bilinear cohesive zone material model for the simulation of the failure of the SRPF in the vicinity of the screw. This adoption enabled the finite elements to detach from each other when the developed interface shear stress reached the value of the shear yield stress of the SRPF.

Adoption of such a "damage law" improved significantly the accuracy of the numerical analysis; on the same time however it added an extra nonlinearity to the problem increasing significantly its complexity and computational requirements. The different mechanical behaviour of a FE model with and without the "damage law" previously described is manifested by the different force-displacement curves shown in Fig.14. As it can be seen from this figure the simplified FE model with Linear Elastic - Perfectly Plastic (LE/PP) SRPF overestimates the pullout force and exhibits an enlarged region of plastic deformations into the SRPF. But the most important disadvantage of this analysis is that the drop of the value of the force that follows its maximum value is caused by sliding of the screw out of the SRPF and not by any sort of failure of the SRPF.

The first conclusion drawn from the numerical analysis was that, when a screw is pulled out of a SRPF block, most of the pullout load is carried by the deepest threads (Fig.7,8). The material surrounding these threads is also indicated to fail first.

Even though the numerically simulated failure of the SRPF is in very good agreement with the experimentally observed one, the prediction that the material in the vicinity of the deepest thread fails first, seems to be inconsistent with the experience and “intuition” of an engineer. Researchers studying threaded connections between metallic parts report a totally different mechanical behaviour. Tafreshi et al.[30] report that the outer-most thread caries most of the pullout load and therefore is the most likely to fail first. Similarly, recently reported results from tests where titanium threaded bars were pulled-out from marble blocks indicated again that the outer-most thread is the worse loaded one [31]. These differences of the mechanical behaviour can be explained by the relative differences in the material properties for these cases (see online supplementary data).

The FE model developed herein was used for the parametric investigation of the influence of the screw’s design on its pullout force. The parameters studied were the outer radius, the inclination, the depth and the pitch of the thread as well as the total number of threads and the purchase length of the screw.

Outer radius is considered to be the most important of these factors. Its significance has been experimentally proven in many cases [7,8,11,13,15-17]. It is even proved (using custom made screws) [8,11,17] that the correlation between the outer radius of a screw and its pullout force is linear. The same conclusion was drawn in the present study.

While the outer radius is considered to be the most important design parameter of a screw’s thread, the inclination of the threads is considered to be among the less important ones. Koranyui et al. [12] studied the holding power of screws with a_1 (Fig.2) angle 0° and 30° using dog femurs and found no statistically significant differences. The present analysis concluded that even though the inclination of the thread does not significantly influence the pullout out force, it influences its dependence on other parameters of the screw’s design, such as the depth and the pitch of the thread.

As far as the depth of the thread is concerned, the results indicated that in the case of sharp threads (a_1=-5°, 5°) a critical value of the thread's depth exists (~0.16% of the screw's outer radius) which renders pullout force practically uninfluenced by any further increase of the depth. This observation is in agreement with the findings of Hughes et al. [14] who studied experimentally the influence of the guiding-hole diameter on the holding power of bone screws. They concluded that the screw's holding power remains practically uninfluenced by the increase of the guiding-hole diameter up to a critical value of 87% of the screw's outer diameter. This observation indicates that the depth of the screws studied by Hughes et al.[14] could be reduced to 13% of their outer radius without changing significantly their pullout force. On the contrary, in the case of less sharp threads (a_1=25°) no critical value of the thread's depth exists. The pullout force was found to increase linearly with increasing depth (Fig.11).

The dependence of the pullout force on the pitch of the screw for different cases of thread's depth was investigated by Asnis et al. [8]. While the authors of this study report strong dependence of the screw's holding power on the value of the pitch, it can be seen from their results that this is the case only for screws with depth equal to 0.75mm. For screws with depths 1.45 and 1.1mm their holding power seems to be uninfluenced by any change of the value of the pitch. De Coster et al. [11] also used custom made screws and concluded that decreasing the value of the screw's pitch from 2.5 to 1mm can significantly increase its pullout force (24% increase). The screws used had depth equal to 0.5mm and also in this case the purchase length was kept constant.

In the present study the influence of the pitch was investigated for constant value of screw purchase length and for different values of the thread's depth and inclination. It was concluded that, in case of relatively small depths (0.5mm) the pitch plays an important role (Fig.12). Smaller values of the pitch can significantly increase the pullout force of the screw. On the contrary for higher depth values (0.75,1mm) the pullout force was practically uninfluenced by any change of the pitch.

Finally, the total number of threads [19] and the purchase length [7] of the screw are reported to be linearly correlated with the screw's pullout force. The same conclusion was also drawn from the present analysis (Fig.13) and this linear correlation was expressed in the form of an empirical equation.

Concerning the limitations of the present study it must be accepted that the phenomenon of hosting material pre-tensioning due to radial compaction was ignored. Radial compaction of the hosting material is observed when the screw is inserted into a hole that is smaller than the screw itself, as it happens in the case of conical screws or screw insertion with under-tapping of the cylindrical guiding hole or without any tapping at all (self-tapping). Radial compaction results in the development of a complex stress field around the screw (before the initiation of the pullout procedure) which is unknown and can not be calculated analytically. The fact that the initial stress state of the hosting material is unknown renders even more difficult the realization of an accurate numerical simulation. In this context and as a first step the present study was focused on cases where the initial stress state of the hosting material is known (i.e. cylindrical screws inserted into SRPF blocks though threaded holes identical to the screws themselves). The FE model presented here, with minor modifications, could be used for a more complete parametric study including cases where the hosting material is radially compacted (e.g. cylindrical screws). Specifically, the challenge of the unknown initial stress state of the hosting material can be met by dividing the simulation into two load steps:

- 1st Step - Pretension: The hosting material is compacted by modifying the geometry and the size of the screw's FE model.
- 2nd Step – Pullout: The screw is pulled out of the hosting material and the pullout force is calculated.

Preliminary results indicated that the above mentioned numerical procedure can satisfactory simulate the influence of radial compaction as this is realized by under-tapping[32].

Additionally synthetic bone, regardless its wide usage, remains an idealization unable to simulate all aspects of the mechanical behaviour of cancelous bone. In any case the value of tests using synthetic bone should not be underestimated since the comparative analysis of the results for different cases can help drawing useful and clinically relevant conclusions. In a recent study[33] with both synthetic and cadaveric bones it was concluded that the "*…patterns of pullout strength and loading energy, as well as statistical significance, were very similar between the two testing models*"[33], although the absolute values of the measured quantities were markedly different.

Another limitation of the present study stems from the imposition of axisymetry. This symmetry assumption restricts the application of the present FE model for more complex loading cases approaching those applied to the pedicle screw in vivo but is acceptable for relatively simple loading cases, as it is pure pullout.

During a pullout test the three-dimensional helicoidal shape of the threads seems to play a minor role concerning the screw's mechanical behaviour. This assumption is supported by many researchers in the literature [19,20,24,30] as well as by the satisfactory agreement between the numerical and experimental results.

On the other hand the main contribution of the present study is the implementation of a unique method for representing the failure in shear of the hosting material surrounding a bone screw.

References

1) Essens S, Sachs B, Dreyzin V. Complications associated with the technique of pedicle screw fixation. A selected survey of ABS members. Spine 1993;18:2231–9.

2) Okuda S, Miyauchi A, Oda T, Haku T, Yamamoto T, Iwasaki M. Surgical complications of posterior lumbar interbody fusion with total facetectomy in 251 patients. J Neurosurg (Spine) 2006;4:304-9.

3) Katonis P, Christoforakis J, Aligizakis AC, Papadopoulos C, Sapkas G, Hadjipavlou A. Complications and Problems Related to Pedicle Screw Fixation of the Spine. Clinical Orthopaedics And Related Research 2003;411:86–94.

4) Rohlmann A, Graichen F, Kayser R, Bender A, Bergmann G. Loads on a telemeterized vertebral body replacement measured in two patients. Spine 2008;33:1170-9.

5) Benzel EC, Implant-Bone interface. In, Biomechanics of spine stabilization. Thieme. 2001;pp:160-161

6) Lyon WF, Cochran JR, Smith L. Actual Holding Power Of Various Screws In Bone. Ann Surg 1941;114:376-384.

7) Chapman J, Harrington R, Lee K, Anderson P, Tencer A, Kowalski D. Factors affecting the pullout strength of cancellous bone screws. J Biomech Eng 1996;118:391-8.

8) Asnis S, Ernberg J, Bostrom M, Wright T, Harrington R, Tencer A, Peterson M. Cancellous Bone Screw Thread Design and Holding Power. J Orthop Trauma 1996;10:462-9

9) Conrad B, Cordista A, Horodyski M, Rechtine GR. Biomechanical evaluation of the pullout strength of cervical screws. J Spinal Disord Tech 2005;18:506–10.

10) Ansell H, Scales J. A study of some factors which affect the strength of screws and their insertion and holding power in bone. J. Biomechanics 1968;1:279-302.

11) DeCoster TA, Heetderks DB, Downey DJ, Ferries JS, Jones W. Optimizing bone screw pullout force. J Orthop Trauma 1990;4(2):169-74.

12) Koranyi E, Bowman C, Knecht C, Janssen M. Holding power of orthopedic screws in bone. Clinical Orthopaedics and Related Research 1970;72:283-6.

13) Thompson J, Benjamin J, Szivek J. Pullout strength of cannulated and noncannulated cancellous bone screws. Clinical Orthopaedics and Related Research 1997;341:241-9.

14) Hughes AN, Jordan BA. The mechanical properties of surgical bone screws and some aspects of insertion practice. Injury 1972;4:25-38.

15) Zindrick M, Wiltse L, Widell E, Thomas J, Holland R, Field T, Spencer C. Biomechanical study of intrapedicular screw fixation in the lumbosacral spine. Clinical Orthopaedics and Related Research 1986;203:99-112.

16) Leggon R, Lindsey RW, Doherty BJ, Alexander J, Noble P. The holding strength of cannulated screws compared with solid screws in cortical and cancelous bone. Journal of Othopaedic Trauma 1993;7:450-7.

17) Gausepohl T, Möhring R, Pennig D, Koebke J. Fine thread versus coarse thread A comparison of the maximum holding power Injury. Int. J. Care Injured 2001;32:SD1–SD7.

18) Krenn M, Piotrowski W, Penzkofer R, AUGAT P. Influence of thread design on pedicle screw fixation: Laboratory investigation. J Neurosurg (Spine) 2008;9:90–5.

19) Zhang QH, Tan SH, Chou SM. Investigation of fixation screw pull-out strength on human spine. Journal of Biomechanics 2004;37:479–485.

20) Zhang QH, Tan SH, Chou SM. Effects of bone materials on the screw pull-out strength in human spine. Medical Engineering & Physics 2006;28:795–801.

21) Gefen A. Optimizing the biomechanical compatibility of orthopaedic screws for bone fracture fixation. Medical Engineering & Physics 2002;24:337–347.

22) Hsu CC, Chao CK, Wang JL, Hou SM, Tsai YT, Lin J. Increase of pullout strength of spinal pedicle screws with conical core: biomechanical tests and finite element analyses. Journal of Orthopaedic Research 2005;23:788–794.

23) Chao CK, Hsu CC, Wang JL, Lin J.Increasing Bending Strength and Pullout Strength in Conical Pedicle Screws: Biomechanical Tests and Finite Element Analyses. J Spinal Disord Tech 2008;21:130–138.

24) Kourkoulis SK, Chatzistergos EP. The influence of the "penetration-" and the "filling- ratios" on the pull-out strength of transpedicular screws. Journal of Mechanics in Medicine and Biology 2009;9:1–18.

25) Long M, Rack HJ. Titanium alloys in total joint replacement--a materials science perspective. Biomaterials 1998;19:1621-39.

26) Dimar J, Glassman S, Puno R, Campbell M, Johnson J. Posterior lumbar spine: CD Horizon Legacy 5.5 Spinal System. In Spinal instrumentation: surgical techniques. Fessler R, Kim D, Vaccaro A, eds. NY:Thieme Medical Publishers Inc,2005:850-5.

27) Alfano G, Crisfield MA. Finite Element Interface Models for the Delamination Anaylsis of Laminated Composites: Mechanical and Computational Issues. International Journal for Numerical Methods in Engineering 2001;50:1701-36.

28) ANSYS, ANSYS Release 11.0 Documentation. ANSYS Inc., Canonsburg, PA, USA.

29) Oberg E, Jones FD, and Horton HL. Working Strength of Bolts. In Machinery's Handbook, Ryffel, HH, ed. Industrial Press, New York, 2004:1509-11.

30) Tafrreshi, A., Dover, W.D., 1993. Stress analysis of drillstring threaded connections using the finite element method. International Journal of Fatigue 15, 429–438.

31) Kourkoulis SK, Papanicolopulos SA, Marinelli A, Vayas I. Restaurierung antiker Tempel: Experimentelle Untersuchungen zum Ausziehverhalten von Verankerungen im Marmor. Bautechnik 2008;85:109-119.

32) Chatzistergos EP, Sapkas G, Kourkoulis SK. The Influence of the Insertion Technique on the Pullout Force of Pedicle Screws: An Experimental Study. Spine (to appear) 2009.

33) Schoenfeld A, Battula S, Sahai V, Vrabec G, Corman S, Burton L, Njus G. Pullout strength and load to failure properties of self-tapping cortical screws in synthetic and cadaveric environments representative of healthy and osteoporotic bone. J Trauma 2008;64:1302–7.

TABLES

Table 1: The values of the quantities which describe the geometry of the threads of the pedicle screws studied (Fig.1).

	CDH 6.5	CDH 7.5	Java TL 5
OR (mm)	*3.25*	*3.75*	*2.5*
CR (mm)	*2.25*	*2.75*	*1.2*
D (mm)	*1*		*1.3*
a_1(°)	*5*		*6*
a_2(°)	*25*		*33*
P (mm)	*2.7*		*1.75*
e (mm)	*0.2*		*0.15*

Table 2: The material properties of the solid rigid polyurethane foam (SRPF) and the titanium alloy of the pedicle screws.

		Tension		Shear	
	Density (gr/cm^3)	Modulus (MPa)	Yield stress (MPa)	Modulus (MPa)	Yield stress (MPa)
SRPF	*0.16*	*57*	*2.2*	*23*	*1.4*
Ti alloy (Ti-6Al-4V) [25,30]	*4430*	110×10^3	*860*	$\sim42\times10^3$	*~500*

Table 3: The parametric design of the numerical study, (*) the respective experimentally measured pullout forces

Parametric study	Outer radius OD (mm)	Core radius CD (mm)	Inclination a_1 (°)	Depth D (mm)	Pitch P (mm)	Number of threads N	Purchace length L (mm)	Pullout Force (N)
OD	2.75	1.75	5	1	2.7	7	18.9	325.7
	3.00	2.00						354.6
	3.25	2.25						382.5/382±3*
	3.75	2.75						439.0/438±2*
a_1	3.75	2.75	-5	1	2.7	7	18.9	435.1
			5					439.0
			15					442.3
			25					446.1
D	3.75	3.25	-5	0.50	2.7	7	18.9	367.7
		3.15		0.60				418.8
		3.00		0.75				428.3
		2.75		1.00				435.1
		2.25		1.50				440.5
		1.75		2.00				443.4
		3.25	5	0.50				367.2
		3.15		0.60				423.5
		3.00		0.75				431.3
		2.75		1.00				439.0
		2.25		1.50				447.1
		1.75		2.00				451.6
		3.25	25	0.50				421.1
		3.15		0.60				430.2
		3.00		0.75				439.1
		2.75		1.00				446.1
		2.25		1.50				458.1
		1.75		2.00				478.6
P	3.75	2.75	25	1.00	1.05	18	18.9	438.9
					1.89	10		451.8
					2.70	7		446.1
					3.15	6		447.0
					3.78	5		442.4
		3.00		0.75	1.05	18		437.7
					1.89	10		447.9
					2.70	7		439.1
					3.15	6		442.2
					3.78	5		433.4
		3.25		0.50	1.05	18		422.2
					1.89	10		422.6
					2.70	7		421.1
					3.15	6		397.4
					3.78	5		281.0
		2.75	5	1.00	0.82	23		436.9
					1.05	18		440.9
					1.89	10		445.2
					2.70	7		439.0
					3.15	6		433.1
					3.78	5		431.8
		3.00		0.75	0.82	23		437.5
					1.05	18		440.2
					1.89	10		444.0
					2.70	7		432.4
					3.15	6		431.7
					3.78	5		427.4
		3.25		0.50	0.82	23		430.1
					1.05	18		431.7
					1.89	10		421.4
					2.70	7		367.2
					3.15	6		327.3
					3.78	5		283.1
N	3.75	2.75	5	1	1	4	4.0	94.0
						5	5.0	115.7
						6	6.0	139.1
						7	7.0	161.0
					1.7	4	6.8	156.3
						5	8.5	196.5
						6	10.2	235.7
						7	11.9	277.4
					2.7	4	10.8	243.6
						5	13.5	308.5
						6	16.2	373.6
						7	18.9	439.0
					3.5	4	14.0	314.1
						5	17.5	398.5
						6	21.0	481.5
						7	24.5	564.8

FIGURE LEGENDS

Fig. 1: The geometry of the FE model of the screw.

Fig. 2: Schematic of the pullout experimental procedure.

Fig. 3: The 2D axisymmetric FE model of the pedicle screw and the SRPF block, (x) is the calibration parameter.

Fig. 4: The bilinear cohesive zone material model [27] which describes the debonding procedure of the bonded contact pairs of Conta171 and Targe169 elements.

Fig. 5: The lines where relative sliding can occur. Taking under consideration the axisymmetric conditions these lines correspond to cylindrical surfaces in three dimensions.

Fig. 6: The experimentally measured and the numerically estimated force-displacement curves for the CDH7.5, CDH6.5 and TL-Java5 screws. For each case the experimental curves correspond to the tests which gave the maximum and minimum pullout force.

Fig. 7: The mechanical behavior of the SRPF – screw system as it is described by the force displacement curve (A) and the Von Mises stress distribution into the SRPF, which lay at the vicinity of the screw, at three different instances (B,C,D) of the pullout test simulation. (B) The imposed displacement is equal to 0.4 mm. (C) The imposed displacement is 0.8 mm and the measured force reaches its maximum value. (D) The maximum achieved displacement (for higher values of displacement the solution doesn't converge).

Fig. 8: The distribution of the pullout load on each thread of the screw for the three instances of the pullout test simulation studied in Fig.7. The threads of the screw are numbered from the outer- to the inner –most one.

Fig. 9: The central section of a specimen after the end of a pullout test and the failure of the SRPF block. In the upper right of the picture the material extracted from the block together with the screw is shown.

Fig. 10: The influence of the inclination of the thread to the distribution of the reaction forces into the SRPF along the slope of the deepest thread. Axis X is parallel to the imposed pullout displacement. The reaction forces correspond to the solution sub-step where the respective force-displacement curve had its maximum force. For all three cases studied CR=2.75mm,OR=3.75mm and P=2.7mm.

Fig. 11: The pullout force for different values of the depth of the thread. The screw OR was kept constant and equal to 3.75mm.

Fig. 12: The pullout forces of screws with varying pitch and thread depths but constant purchase length (18.9mm). (A) a_1=5º, (B) a_1=25º.

Fig. 13: The pullout forces of screws with 4-7 total number of threads and pitch 1-3.5mm. For every case the depth of the threads was 1mm and their a_1 angle 5°.

Fig. 14. Comparison of the force-displacement curves calculated by the FE model developed here (LE/PP+Damage law) and by a FE model where the SRPF is simulated simply as a linear elastic perfectly plastic material (LE/PP).

FIGURES

Figure 1

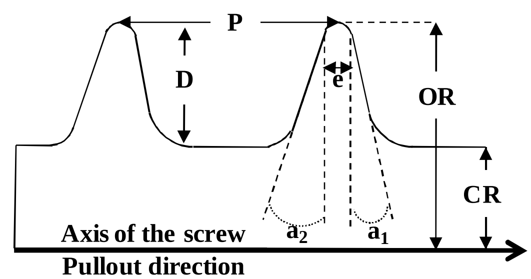

Figure 2

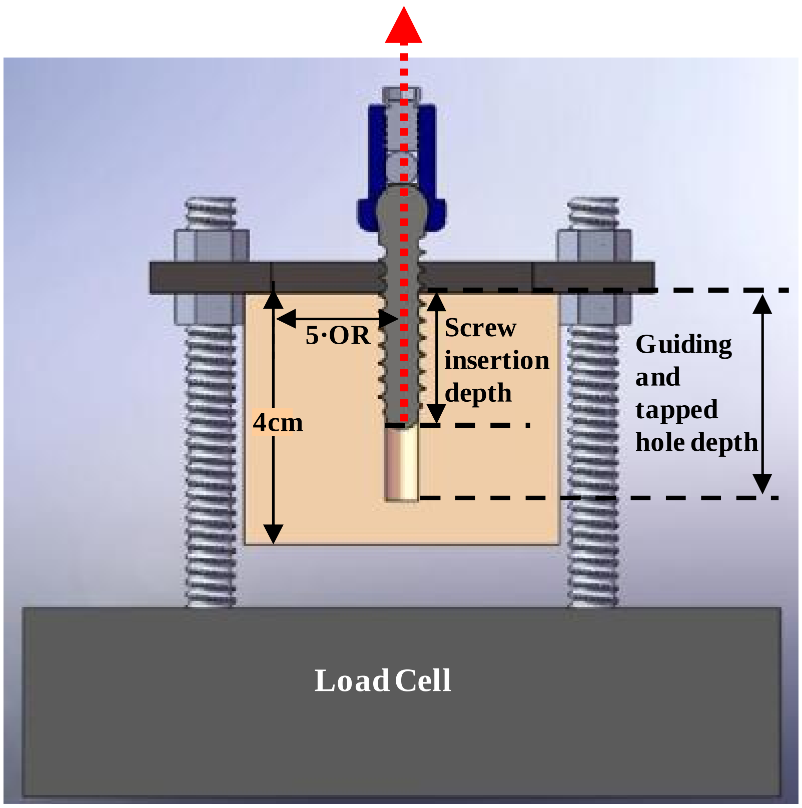

5·OR
Screw insertion depth
Guiding and tapped hole depth
4cm
Load Cell

Figure 3

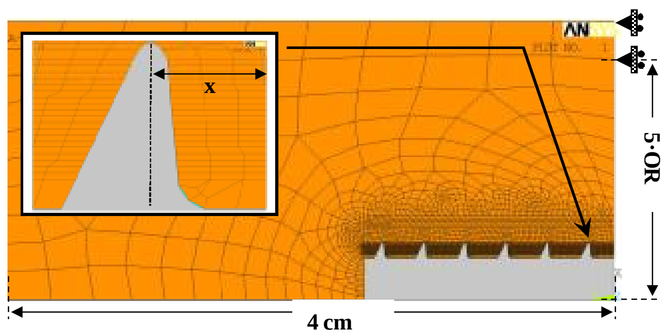

Figure 4

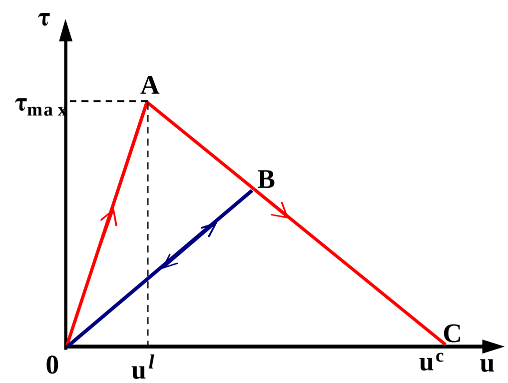

Figure 5

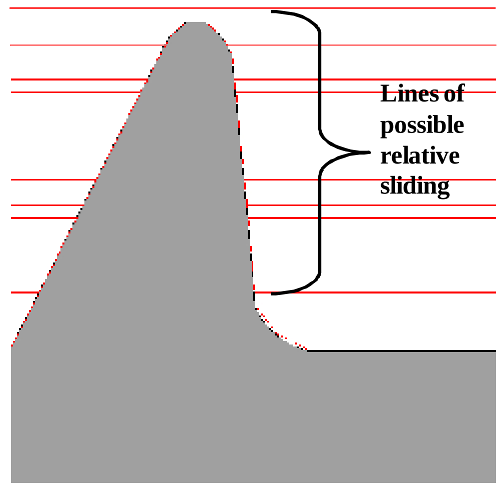

Figure 6

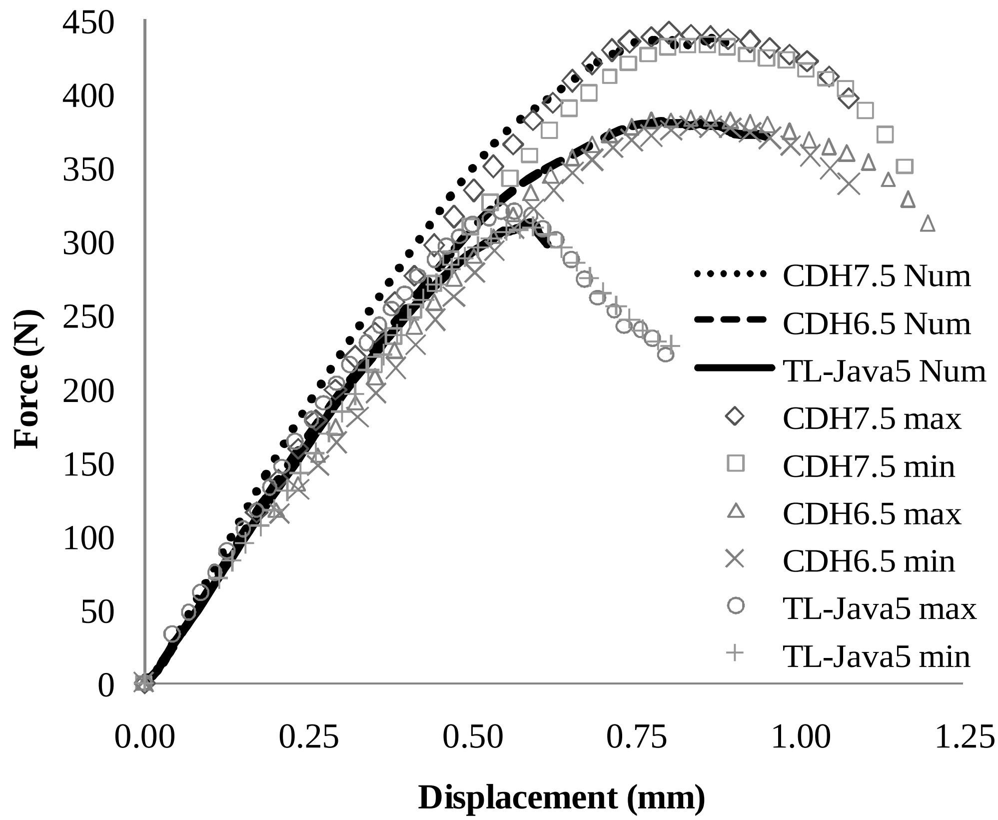

450
400
350
300
250
200
150
100
50
0
Force (N)
0.00
0.25
0.50
0.75
1.00
1.25
Displacement (mm)
CDH7.5 Num
CDH6.5 Num
TL-Java5 Num
CDH7.5 max
CDH7.5 min
CDH6.5 max
CDH6.5 min
TL-Java5 max
TL-Java5 min

Figure 7

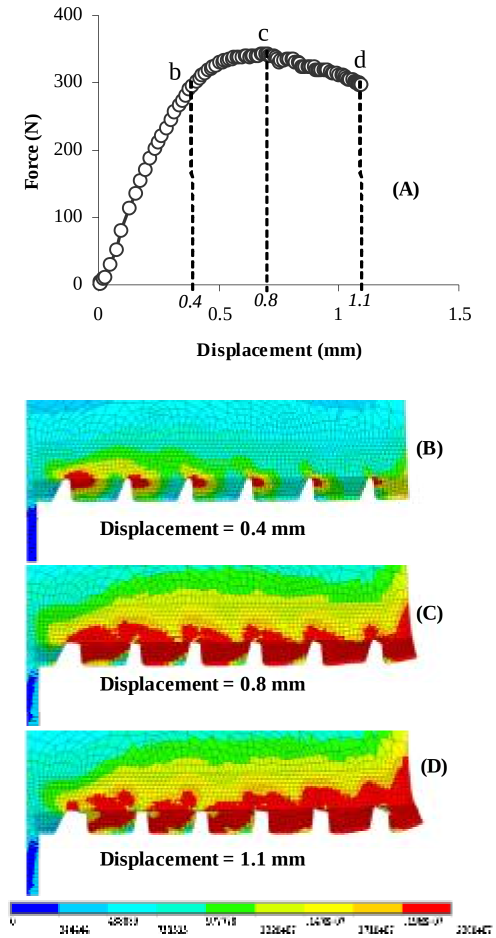

400
300
200
100
0
Force (N)
b
c
d
(A)
0.4
0.8
1.1
0
0.5
1
1.5
Displacement (mm)
(B)
Displacement = 0.4 mm
(C)
Displacement = 0.8 mm
(D)
Displacement = 1.1 mm

Figure 8

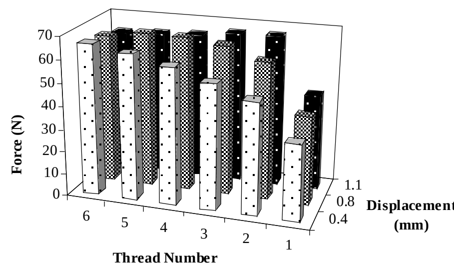
70
60
50
40
30
20
10
0
Force (N)
6
5
4
3
2
1
Thread Number
1.1
0.8
0.4
Displacement (mm)

Figure 9

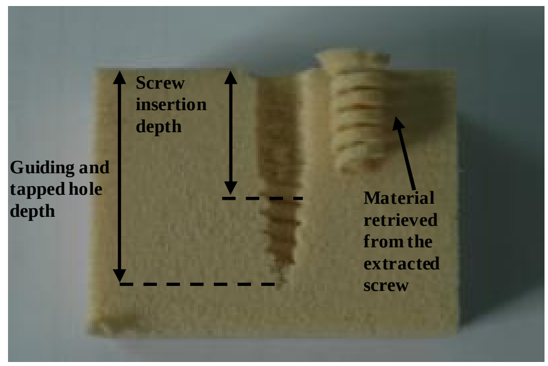

Screw insertion depth
Guiding and tapped hole depth
Material retrieved from the extracted screw

Figure 10

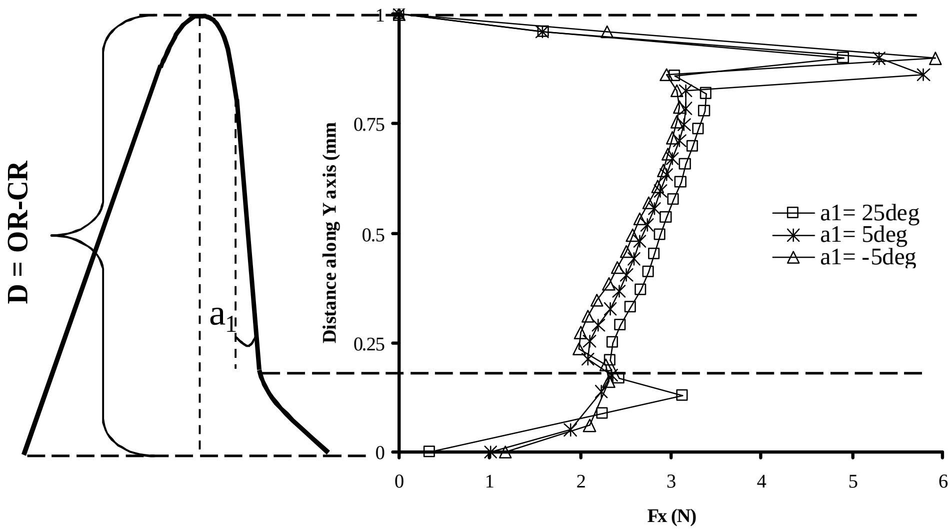

D = OR-CR
a1
Distance along Y axis (mm
Fx (N)
a1= 25deg
a1= 5deg
a1= -5deg
1
0.75
0.5
0.25
0
0
1
2
3
4
5
6

Figure 11

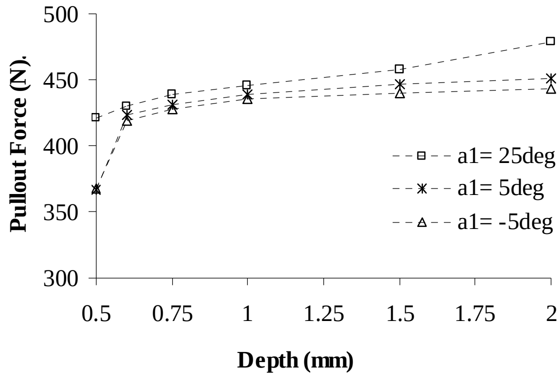

500
450
400
350
300
Pullout Force (N).
0.5
0.75
1
1.25
1.5
1.75
2
Depth (mm)
a1= 25deg
a1= 5deg
a1= -5deg

Figure 12

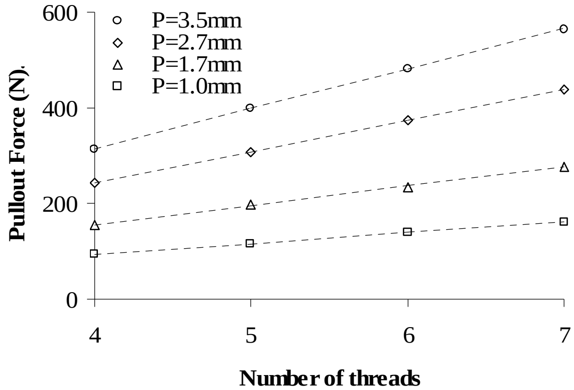

600
400
200
0
4
5
6
7
Pullout Force (N)
Number of threads
P=3.5mm
P=2.7mm
P=1.7mm
P=1.0mm

Figure 13

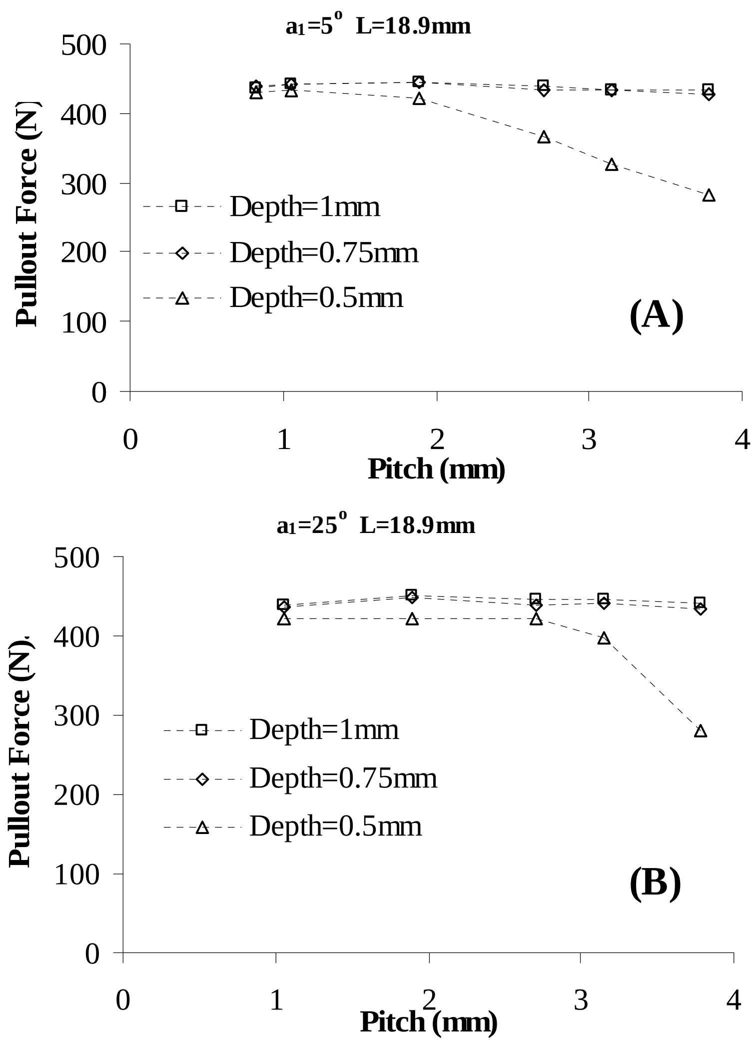

a1=5° L=18.9mm
Pullout Force (N)
500
400
300
200
100
0
Depth=1mm
Depth=0.75mm
Depth=0.5mm
(A)
0
1
2
3
4
Pitch (mm)
a1=25° L=18.9mm
Pullout Force (N)
500
400
300
200
100
0
Depth=1mm
Depth=0.75mm
Depth=0.5mm
(B)
0
1
2
3
4
Pitch (mm)

Figure 14

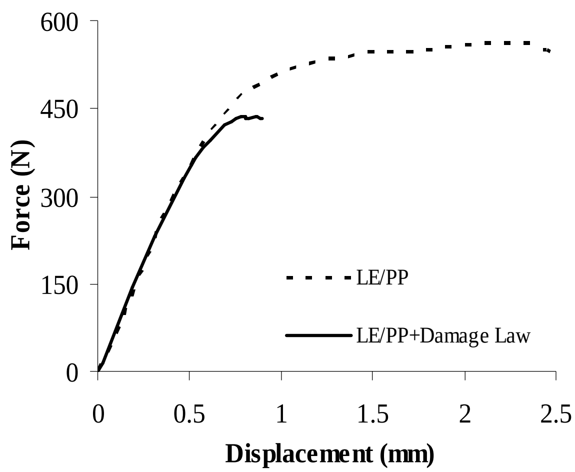
600
450
300
150
0
Force (N)
0
0.5
1
1.5
2
2.5
Displacement (mm)
LE/PP
LE/PP+Damage Law